

Article

In Vitro Evaluation and Genome Mining of *Bacillus subtilis* Strain RS10 Reveals Its Biocontrol and Plant Growth-Promoting Potential

Sajid Iqbal, Nimat Ullah  and Hussnain Ahmed Janjua *

Department of Industrial Biotechnology, Atta-ur-Rahman School of Applied Biosciences (ASAB), National University of Sciences and Technology (NUST), H-12, Islamabad 44000, Pakistan; siqbal.phdabs12asab@asab.nust.edu.pk (S.I.); nullah.phdabs12asab@asab.nust.edu.pk (N.U.)

* Correspondence: hussnain.janjua@asab.nust.edu.pk; Tel.: +92-32-3568-0231

Abstract: Recently, crop management has involved excessive use of chemical fertilizers and pesticides, compromising public health and environmental integrity. Rhizobacteria, which can enhance plant growth and protect plants from phytopathogen, are eco-friendly and have been attracting increasing attention. In the current study, *Bacillus subtilis* RS10 isolated from the rhizosphere region of *Cynodon dactylon*, inhibited the growth of indicator strains and exhibited in vitro plant growth-promoting traits. A whole-genome analysis identified numerous biosynthetic gene clusters encoding antibacterial and antifungal metabolites including bacillibactin, bogorol A, fengycin, bacteriocin, type III polyketides (PKs), and bacilysin. The plant growth-promoting conferring genes involved in nitrogen metabolism, phosphate solubilization, hydrogen sulfide, phytohormones, siderophore biosynthesis, chemotaxis and motility, plant root colonization, lytic enzymes, and biofilm formation were determined. Furthermore, genes associated with abiotic stresses such as high salinity and osmotic stress were identified. A comparative genome analysis indicated open pan-genome and the strain was identified as a novel sequence type (ST-176). In addition, several horizontal gene transfer events were found which putatively play a vital role in the evolution and new functionalities of a strain. In conclusion, the current study demonstrates the potential of RS10 antagonism against important pathogens and plant growth promotion, highlighting its application in sustainable agriculture.

Keywords: whole-genome sequence; *Bacillus subtilis* novel ST176; pan-/core-genome analysis; antibacterial activity; plant growth-promoting bacteria (PGPB); sustainable agriculture



Citation: Iqbal, S.; Ullah, N.; Janjua, H.A. In Vitro Evaluation and Genome Mining of *Bacillus subtilis* Strain RS10 Reveals Its Biocontrol and Plant Growth-Promoting Potential.

Agriculture **2021**, *11*, 1273. <https://doi.org/10.3390/agriculture11121273>

Academic Editors: Tibor Szili-Kovács and Tünde Takács

Received: 8 October 2021

Accepted: 1 December 2021

Published: 15 December 2021

Publisher's Note: MDPI stays neutral with regard to jurisdictional claims in published maps and institutional affiliations.



Copyright: © 2021 by the authors. Licensee MDPI, Basel, Switzerland. This article is an open access article distributed under the terms and conditions of the Creative Commons Attribution (CC BY) license (<https://creativecommons.org/licenses/by/4.0/>).

1. Introduction

Bacterial strains that efficiently colonize plant roots and promote plant growth by direct or indirect mechanisms are known as plant growth-promoting bacteria (PGPB) [1]. The direct mechanism includes stimulation of root growth and biofertilization, while the indirect mechanism involves biological control comprised of induction of systemic resistance and production of antimicrobial metabolites [2]. *Bacillus* spp. are considered to be promising PGPB due to their endospore-forming capabilities, which enable them to better survive in a diverse habitat [3], their antimicrobial potential, and most importantly their abundant plant growth-promoting traits such as phosphate solubilization, nitrogen fixation, and sulfur oxidation [2]. Antimicrobial metabolites produced by *Bacillus* spp. are extremely diverse [4]. According to their biosynthetic pathways, these antimicrobial metabolites can be divided into three main classes: nonribosomal peptides (NRPs), polyketides (PKs), and ribosomally synthesized post-translationally modified peptides (RiPPs) [5]. NRPs such as surfactin and fengycin are synthesized by mega enzymes called nonribosomal peptide synthetases (NRPSs). NRPSs are constituted of various modules and each module incorporates a single amino acid residue. PKs include bacillaene and difficidin is another class of antimicrobial metabolites synthesized by polyketide synthetases (PKSs). Unlike

NRPs and PKs, RiPPs (bacteriocin) is a class of antimicrobial metabolites synthesized in a normal ribosomal fashion. The antimicrobial metabolites produced by *Bacillus* spp. play an important role in biological control. For instance, the knockout of NRPs (surfactin) synthesis genes in *B. subtilis* strain 6051 reduce its potential to colonize plant roots and to protect the plant against phytopathogens [6]. Fengycins and iturins produced by *B. subtilis* inhibit the growth of pathogenic *Podospaera fusca*, which causes disease in seasonal plant leaves [7]. Similarly, *B. velezensis* strain FZB42 produces bacilysin, bacillaene, and difflidin which suppress fire blight disease in plants [8]. Recently, it was reported that *B. subtilis* SL18r and *B. simplex* Sneb545 elicit induce systemic resistance in plants against *Botrytis cinerea* and *Heterodera glycines*, respectively [9,10]. Furthermore, volatile organic compounds such as acetoin and 2,3-butanediol have also been reported to trigger systemic resistance in plants [11]. In the past, several studies focused on PGPB, however, their antimicrobial activities were limited to phytopathogens and they neglected the animal pathogens that can enter the animal body by grazing. For instance, a fungal pathogen, *C. purpurea*, causes ergotism in humans, and ruminants are originated from plants [12]. *P. chartarum*, which is another fungal pathogen that causes sinusitis and rhinitis in horses [13], also emerges from plants. PGPB which antagonizes both mammalian and phytopathogens would ensure safety of the food chain. Therefore, the current study was designed to isolate and evaluate *Bacillus* spp. for plant growth-promoting/antimicrobial activity against important pathogens and further genome mining to explore the cryptic genomic potential that contributes to sustainable agriculture.

2. Materials and Methods

2.1. Strain Isolation and Antimicrobial Activity Assay

Soil samples (10 g, n = 12) were collected from various rhizosphere regions including peanuts, Bermuda grass, maize, grapes, and wheat rhizosphere of Kohat division, KP, Pakistan. A series of dilutions were prepared to start with 1 g of sample in 10 mL sterile phosphate buffer solution. With 100 µL from each dilution spread on trypticase soy agar (Oxide, UK), the plates were sealed and incubated at 30 °C for 24 h. The strain RS10 was isolated from a soil sample collected from the *Cynodon dactylon* rhizosphere at the depth of 2–5 cm in May 2018 from the southern region (33.1105, 71.0914) of Khyber Pakhtunkhwa, Pakistan. The isolated strains were preliminarily screened for antibacterial activities, as described earlier [14]. Subsequently, the antibacterial activity of the strain RS10 culture extract was determined against a set of American Type Culture Collection (ATCC) strains (*Streptococcus pneumoniae* 6305, *Pseudomonas aeruginosa* 15442, *Staphylococcus aureus* 6538, *Escherichia coli* 8739, *Salmonella typhimurium* 14028, *Listeria monocytogenes* 13932, *Pseudomonas syringae* 21721, and *Klebsiella pneumoniae* 13889). Briefly, the strain RS10 was incubated in tryptic soy broth at 30 °C for 48 h and 500 mL cell-free supernatant was obtained by centrifugation at 15,000× g for 15 min at 4 °C. The cell-free supernatant was extracted twice using an equal volume of ethyl acetate (1:1) and antibacterial metabolites were concentrated in a rotary evaporator at 60 °C until ethyl acetate was completely evaporated. The dry extract was dissolved in phosphate buffer solution (250 mg/mL) and antibacterial activity was determined against a set of ATCC bacterial strains via agar well diffusion assay and zones of inhibitions (ZOI) were measured in mm [15]. Penicillin and Gentamicine were used as positive control against Gram-positive and Gram-negative ATCC strains, respectively.

For antifungal activity, a 6 mm mycelial plug was picked from two actively growing phytopathogenic fungi (*Botrytis cinerea* strain KST-32 and *Aspergillus niger* strain MB-4) and placed in the middle of the petri plate containing potato dextrose agar (PDA). The partially purified extract (200 µL) of RS10 was poured near the edge of the plate and incubated for 7 days at 25 °C. The petri plate containing only mycelial disc at the center incubated at the same condition was used as a positive control. The growth of inhibition was determined using the following formula:

$$GI\% = \frac{C - T}{C} \times 100$$

where GI represents growth inhibition, C is the diameter in control, and T is the diameter in treated (RS10 extract).

2.2. *In Vitro Plant Growth-Promoting Assay*

The strain RS10 was spot inoculated on a phosphate agar plate containing (g/L) yeast extract 0.5, dextrose 10, calcium phosphate 5, ammonium sulfate 0.5, sodium chloride 0.2, potassium chloride 0.2, ferrous and manganese sulfate 0.0001 g, magnesium sulfate 0.1, and agar 12. The plate was incubated at 30 °C for 48 h. Colonies showing clear halo zones indicated phosphate solubilization activity. Biofilm synthesis was determined through calorimetric assay, as described earlier [16]. The absorbance was taken as an index of biofilm synthesis and 33% acetic acid in water was used as a negative control. The extracellular proteases and cellulase production were assessed, according to the method reported previously [17]. Siderophore production was evaluated using a modified microplate assay, as described earlier [18].

2.3. *DNA Extraction, Whole-Genome Sequencing, Assembly, and Annotation*

The genomic DNA was extracted from a fresh broth culture using a pure link genomic DNA extraction kit (Invitrogen Carlsbad, USA). The quantity and quality of isolated genomic DNA was estimated using a Nanodrop spectrophotometer (Titertek Berthold, Pforzheim, Germany). The genomic DNA library was prepared using a Nextera XT library preparation kit (Illumina Inc. San Diego, CA, USA) and was sequenced using a HiSeq Illumina 2500 platform with paired-end reads. The reads were trimmed using trimmomatic v 0.36 [19] and de novo assembly was performed with SPAdes v 3.12 [20]. Gaps within the scaffolds were closed, as described earlier [21]. Genome annotation was performed through the NCBI's Prokaryotic Genome Annotation Pipeline (PGAP) version 4.10 [22]. CGview online server (<http://cgview.ca/>, accessed on 25 September 2021) was used to generate a circular map of strain RS10 for comparison with the reference genome.

2.4. *Taxonomic Investigation and Genome Characterization of Strain RS10*

To determine the exact taxonomic position of the strain, multilocus sequence type (MLST) analyses was performed. The MLST 2.0 online web server (<https://cge.cbs.dtu.dk/services/MLST/>, accessed on 15 January 2020) was used to identify the sequence type for strain RS10. To verify a unique sequence type, the allelic profiling of seven housekeeping genes (glpF91, ilvD3, pta103, purH112, pycA96, rpoD1, and tpi63) were submitted to the PubMLST database (<https://pubmlst.org/b subtilis/>, accessed on 23 January 2020). The rapid annotation subsystem technology (RAST) approach was used to categorize the genes coding for a set of proteins involved in a specific biological process. Genomic islands (GIs) were predicted using an online Islandviewer 4 server (<http://www.pathogenomics.sfu.ca/islandviewer/>, accessed on 12 September 2021) and prophage regions were identified with the PHASTER online search tool (<https://phaster.ca/>, accessed on 15 September 2021).

2.5. *Genome Mining for Synthesis of Bioactive Compounds*

To identify putative secondary metabolites BGCs, *B. subtilis* RS10 genome was submitted to Antibiotics and Secondary Metabolites Analysis Shell (AntiSMASH) (<https://antismash.secondarymetabolites.org/>, accessed on 20 September 2021). Furthermore, gene similarity with known clusters and domain functions were identified and annotated using BLASTp and Pfam analysis.

2.6. *Pan- and Core-Genome Estimation and Phylogenetic Analysis*

Currently (January 2021), 382 *B. subtilis* genome assemblies are available in public databases. However, most of these are draft or partial genome sequences. Therefore, we selected only the complete (139) genomes of *B. subtilis* for the Pan-/core-genome analysis. For this course, Bacterial Pan Genome Analysis (BPGA-V-1.3) pipeline was used by applying default parameters [23]. A set of genes shared by all strains were defined

as core-genome, a set of genes shared by more than 2 strains was defined as accessory genes, and a set of genes that were specific to a single strain was defined as unique genes and the entire gene contents of the targeted genomes were defined as pan-genome. The concatenated core-genomes were aligned using Clustal Omega server (<https://www.ebi.ac.uk/Tools/msa/clustalo/>, accessed on 13 March 2021) and a core-genome-based maximum likelihood (ML) phylogenetic tree was constructed using MEGAX [24]. The tree was edited and annotated using iTOL (<https://itol.embl.de/>, accessed on 25 March 2021).

2.7. Availability of Data

The whole-genome sequence of *B. subtilis* strain RS10 has been submitted to NCBI, GenBank under the accession number CP046860.1. The BioSample and BioProject were registered under accession numbers SAMN13510061 and PRJNA594265, respectively.

3. Results

3.1. Phenotypic Characterization and Antimicrobial Activity

A total of 104 putative *Bacillus* spp. were isolated from various localities and evaluated for antibacterial and plant growth-promoting activities. Among these, 12 isolates showed antibacterial activities against at least two indicator strains (Supplementary File S1 Table S1) among all RS10 exhibited strong antagonistic activity as well as plant growth-promoting traits; and therefore were selected for further study. The partially purified metabolites extract of strain RS10 also showed promising activity against all indicator ATCC strains. The maximum antibacterial activity was observed against *S. aureus* (14 ± 0.5) followed by *L. monocytogenes* (13.6 ± 0.57) and *P. syringae* (13.33 ± 0.57) (Figure 1A). The strain RS10 also showed antifungal activity against *B. cinerea* and *A. niger* with growth inhibition of 31.25% and 37.5%, respectively.

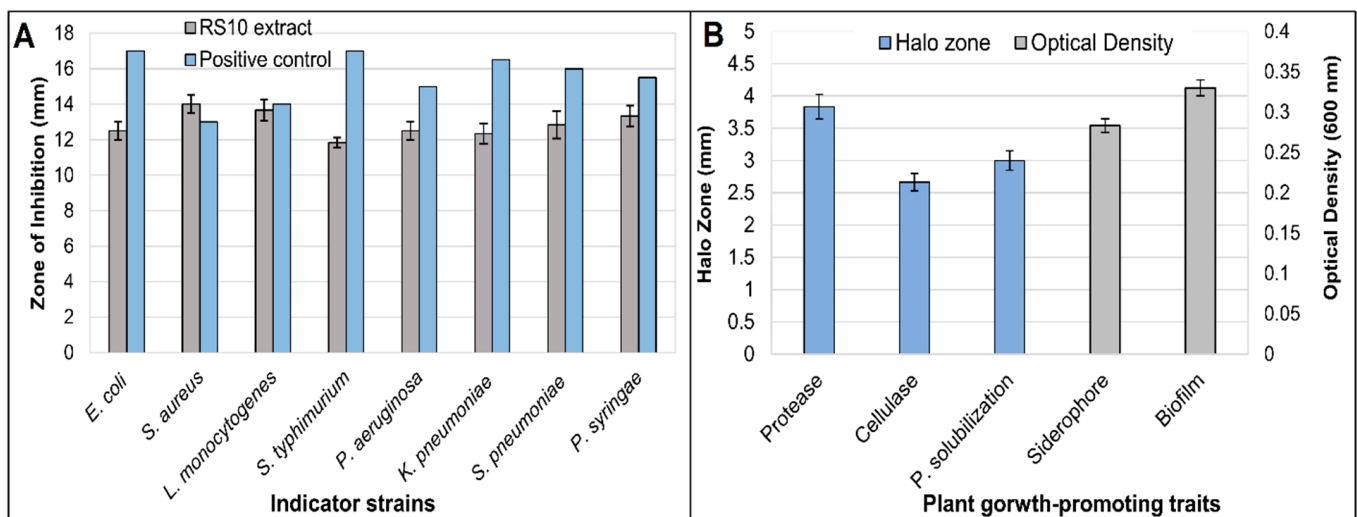


Figure 1. (A) Antibacterial activity of culture extract against indicator ATCC strains; (B) plant growth-promoting ability of *B. subtilis* strain RS10. The bar graph represents mean values \pm standard deviation of triplicates experiments.

3.2. In Vitro Plant Growth-Promoting Traits

The in vitro screening of strain RS10 showed positive results for all tested plant growth-promoting traits. Clear halo zones of 3 ± 0.5 mm, 3.8 ± 0.28 mm, and 2.6 ± 0.28 mm were observed around the colonies for phosphate solubilization, protease, and cellulase production, respectively. The OD values at 600 nm for siderophore synthesis and biofilm formation were 0.28 ± 0.015 and 0.32 ± 0.01 , respectively (Figure 1B). While the values for negative control did not exceed 0.025.

3.3. Whole-Genome Sequence and Annotations

A total of 7,21,782 reads were obtained, resulting in ~45x coverage of the RS-10 genome. The reads were filtered and assembled in 17 scaffolds with a N50 value of 21,73,521 and a L50 of one. Gaps within the scaffold were closed and contigs less than 500 bp were excluded which result in a high-quality, single scaffold draft genome. The RS10 genome is 4,457,201 bp in size with 43.4% G + C content, 5025 genes, 4232 CDS, 86 tRNAs, 11 rRNAs, and five ncRNAs. The whole-genome sequence of *B. subtilis* RS10 is presented in a circular map as compared with a reference strain, i.e., *B. subtilis* strain 168 (Figure 2).

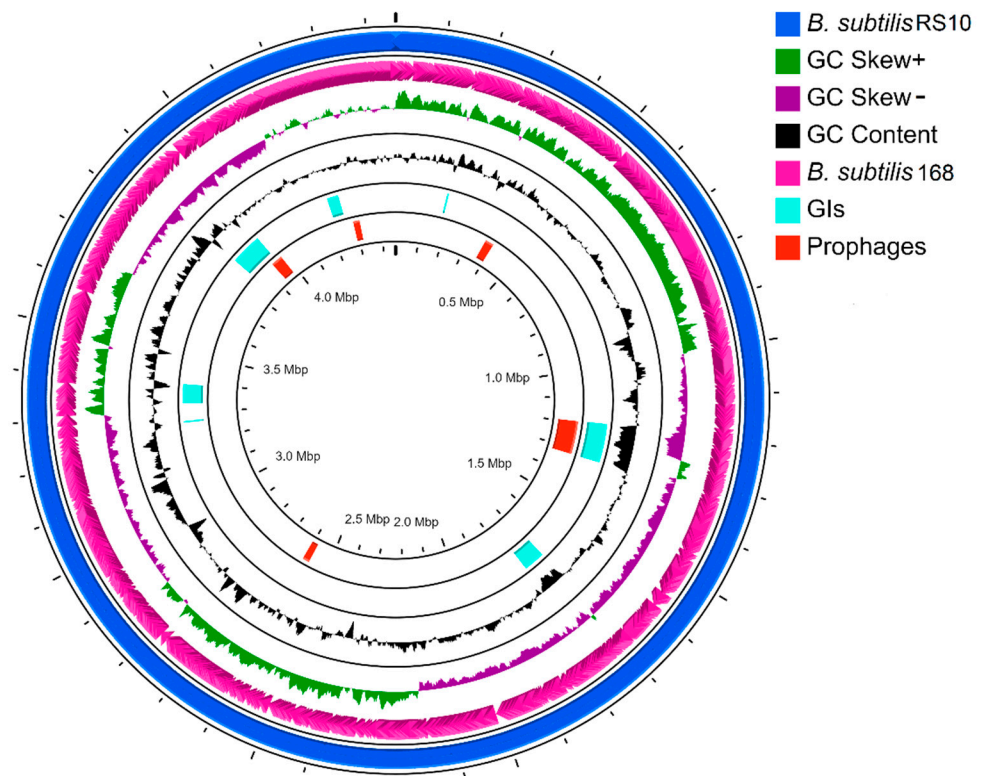


Figure 2. Circular map of the *B. subtilis* strain RS10 genome. The outermost two circles represent the open reading frame (ORFs) of *B. subtilis* RS10 and *B. subtilis* 168, followed by GC content (black). Purple and green colors represent negative and positive strands, respectively. Circle 5th and 6th representing the genomic location of genomic islands (GIs) and prophages, respectively.

3.4. Characterization of Genome

The *B. subtilis* strain RS10 was identified as unknown by MLST 2.0 online server and predicted as a unique multilocus sequence type (MLST). The allelic profile of seven house-keeping genes (*glpF91*, *ilvD3*, *pta103*, *purH112*, *pycA96*, *rpoD1*, and *tpi63*) was submitted to the PubMLST database and the new sequence type ST176 was obtained.

The RAST subsystem analysis revealed the following: 371 genes involved in amino acid and its derivatives metabolism, 289 genes involved in carbohydrate metabolism, 226 genes involved in protein metabolism, 50 genes involved in stress response, 53 genes involved in membrane transport, 55 genes involved in motility and chemotaxis, 96 genes involved in cell wall and capsule, 74 genes involved in RNA metabolism, and 162 genes involved in cofactors, prosthetic group, vitamins and pigment synthesis (Figure 3).

IslandViewer 4 identified 23 GIs in the strain RS10 genome, however, we considered the GIs (7) which were predicted by at least two of three tested methods (IslandPath-DIMOB, SIGE-HMM, and IslandPick) (Figure 2). The identified GIs contains genes associated with carbohydrate and amino acid metabolism, cellular process, biosynthesis of antibacterial compounds, prophage, stress response, xenobiotics degradation, information

process, and numerous genes with unknown function (Supplementary File S2 Table S1). Furthermore, five prophage regions including two intact prophages were predicted in RS10 genome. The two intact prophage genome sizes are 33.6 (44.83 GC%) and 129.3 kb (34.70 GC%) coding 46 and 175 CDS, respectively. The intact prophage-1 exhibited the highest similarity with phage Jimmer2 (NC_041976), while intact phage-2 showed high similarity with SPbeta phage (NC_001884). The two incomplete prophages are 27.1 and 25.3 kb in size and carry 13 and 33 coding sequences, respectively. The questionable prophage is 45 kb in size and contains 66 coding sequences (Supplementary File S2 Table S2). The genes identified in prophages are mostly unknown and some are associated with important enzymes such as endonucleases, recombinases/integrases, and transcriptional regulators.

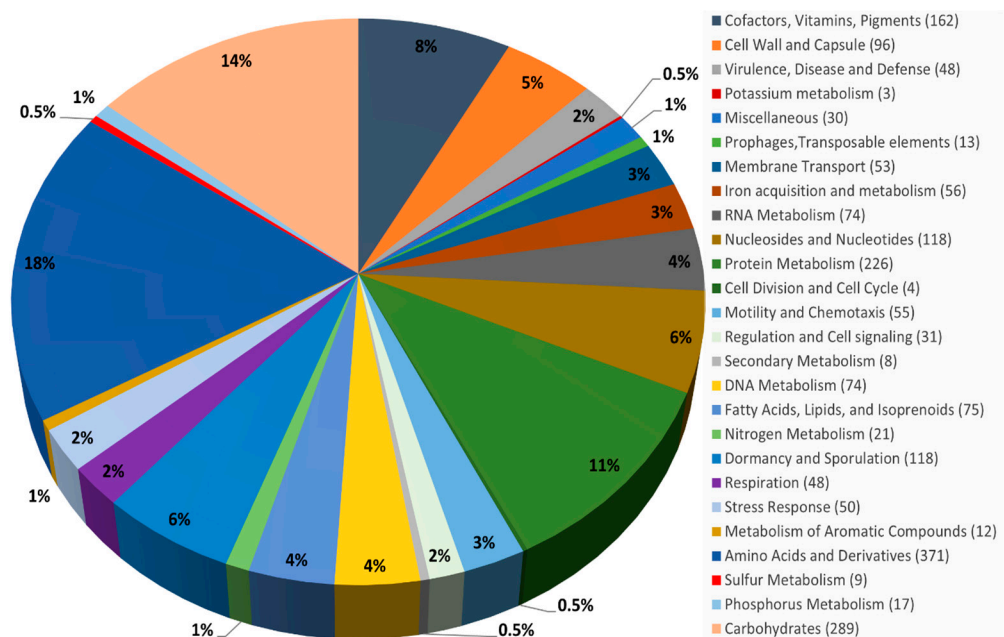


Figure 3. Subsystem category distribution and the biological function of *B. subtilis* strain RS10 based on RAST genome analysis. The distributions of genes are represented with different colors and their corresponding genes are numerically shown within parenthesis.

3.5. Genome Mining for Synthesis of Bioactive Compounds

The AntiSMASH analysis revealed a total of 12 secondary metabolite BGCs composed of 5 putative NRPS including one each for fengycin, bacillibactin, and bogorol A and two putative NRPS for surfactin biosynthesis, 2 putative BGCs each for terpenes and RiPP i-e sectipeptide and bacteriocin, respectively, and one cluster each for type III Polyketide synthase (PKS), hybrid (NRPS + PKS), and bacilycin in the RS10 genome (Table 1).

The four BGCs encoding for antibacterial metabolites (bacillaene, bacilycin, subtilisin, and bacilycin), and one cluster coding for antifungal metabolite (fengycin) exhibit 100% similarity with known gene clusters. While the 2 surfactin BGCs in strain RS10 exhibit 82% and 13% similarity with BGCs (BGC0000433) encoded by *B. velezensis* strain FZB42. The strain RS10 carried a unique BGC and showed 27% gene similarity with bogorol A (BGC0001532) produced by *Brevibacillus laterosporus* and 18% similarity with a Gram-negative antibiotic brevicidin. The current study also identified two unique clusters coding for terpenes. In addition, one BGC each for T3PKS and bacteriocin were also found unique and did not showed similarity with any known clusters (Figure 4).

Table 1. Comparison of biosynthetic gene clusters (BGCs) in the *Bacillus subtilis* strain RS10 and the reference strain *B. subtilis* 168 (CP053102.1).

<i>B. subtilis</i> Strain	Type	from-to (Location)	Similar Known Cluster	Similarity (%)	MiBIG Accession	Core Genes/Product	Locus Tag
<i>B. subtilis</i> strain RS10	Terpene	200,088–220,597	-	-	-	<i>farP</i> <i>pksM</i> , <i>pksL</i> , <i>pksJ</i> , <i>pksF</i> , <i>pabD</i> <i>ppsA</i> , <i>ppsB</i> , <i>ppsC</i> , <i>ppsD</i> , <i>ppsE</i>	GPJ55_01150 GPJ55_04475, GPJ55_04470, GPJ55_04465, GPJ55_04445, GPJ55_04435 GPJ55_05125, GPJ55_05120, GPJ55_05115, GPJ55_05110, GPJ55_05105
	NRPS/PKS (Hybrid)	811,852–926,624	Bacillaene	100	BGC0001089		
	NRPS	991,179– 1,073,561	Fengycin	100	BGC0001095		
	Terpene	1,135,043– 1,156,941	-	-	-	<i>sqhC</i>	GPJ55_05630
	T3PKS	1,333,347– 1,374,462	-	-	-	Type III PK synthase	GPJ55_06995
	RiPP	2,182,762– 2,204,373	Subtilosin	100	BGC0000602	<i>albA</i>	GPJ55_11595
	NRPS	2,732,417– 2,781,432	Bacillibactin	100	BGC0000309	<i>dhbF</i>	GPJ55_14440
	RiPP-like	3,130,241– 3,140,627	-	-	-	Lactococcin_972	GPJ55_16320
	NRPS	3,060,360– 3,123,912	Surfactin	82	BGC0000433	<i>srfAA</i> , <i>srfAB</i> , <i>srfAC</i>	GPJ55_16175, GPJ55_16170, GPJ55_16165
	Others	3,621,808– 3,661,798	Bacilycin	100	BGC0001184	<i>bacD</i>	GPJ55_18880
	NRPS	4,134,934– 4,193,216	Bogorol A	27	BGC0001532	AMP binding D	GPJ55_21740
	Other	4,292,650– 4,333,087	Zwittermicin A	14	BGC0001059	ATP-grasp D	GPJ55_23355
	NRPS	4,365,207– 4,413,851	Surfactin	21	BGC0000433	AMP-binding D	GPJ55_24185, GPJ55_24285
<i>B. subtilis</i> strain 168	RiPP (Sectipeptide)	204,184–226,257	Sporulation killing factor	100	BGC0000601	<i>skfC</i> ,	HIR77_01215, HIR77_01210
	NRPS	358,312–421,753	Surfactin (Lipopeptide)	82	BGC0000433	<i>srfAA</i> , <i>srfAB</i> , <i>srfAC</i> <i>fabD</i> , <i>pksF</i> , <i>pksJ</i> , <i>pksL</i> , <i>pksM</i> <i>ppsE</i> , <i>ppsD</i> , <i>ppsC</i> , <i>ppsB</i> , <i>ppaA</i>	HIR77_02010, HIR77_02015, HIR77_02020 HIR77_09265, HIR77_09285, HIR77_09305, HIR77_09310, HIR77_09315 HIR77_09915, HIR77_09920, HIR77_09925, HIR77_09930, HIR77_09935
	NRPS/PKS (Hybride)	1,763,795– 1,878,554	Bacillaene	100	BGC0001089		
	NRPS (Beta-lactone)	1,935,481– 2,017,771	Fengycin	100	BGC0001095		
	RiPP (Glycocin)	2,371,880– 2,392,050	Sublancin	100	BGC0000558	<i>sunA</i>	HIR77_12430
	RiPP (Sectipeptide)	3,926,529– 3,948,140	Subtilosin	100	BGC0000602	<i>albA</i>	HIR77_20830
	Others	3,951,139– 3,992,557	Bacilycin	100	BGC0001184	<i>bacD</i>	HIR77_21005
	Terpene	2,092,203– 2,114,101	-	-	-	<i>sqhC</i>	HIR77_10505
	Terpene	1,149,982– 1,170,501	-	-	-	<i>farP</i>	HIR77_05960
	T3PKS	2,409,316– 2,450,431	-	-	-	Type III PK synthase	HIR77_12750
	NRPS	3,373,534– 3,423,275	Bacillibactin	100	BGC0000309	<i>dhbF</i>	HIR77_18050

Key. -, similarity not found; NRPS, Nonribosomal peptide synthetase cluster; PKS, polyketide synthase cluster; T3PKS, Type 3 polyketide synthase; RiPP, ribosomally synthesized and post-translational modified peptides.

3.6. Plant Growth-Promoting Capabilities

3.6.1. Nitrogen Metabolism and Phosphate Solubilization

On the one hand, the genome of *B. subtilis* strain RS10 lacks the genes responsible for nitrogen fixation (*nif*) main component. However, the strain contains several genes essential for assimilatory and dissimilatory nitrate and nitrite reduction pathways. These include *nasABCDE* and *nirD* genes. Furthermore, nitrate and nitrite transport-related genes *narGHIJK* were also detected (Supplementary File S3 Table S1). On the other hand, complete machinery for phosphate solubilization was found. In addition, phosphatase

(*phoAD*), which hydrolyze phosphomonoester and catalyze the phosphoryl reaction in the presence of a specific phosphate receptor were identified in RS10 genome. Additionally, genes involved in phosphate transport (*pstACS*) were also identified in RS10 genome (Supplementary File S3 Table S1).

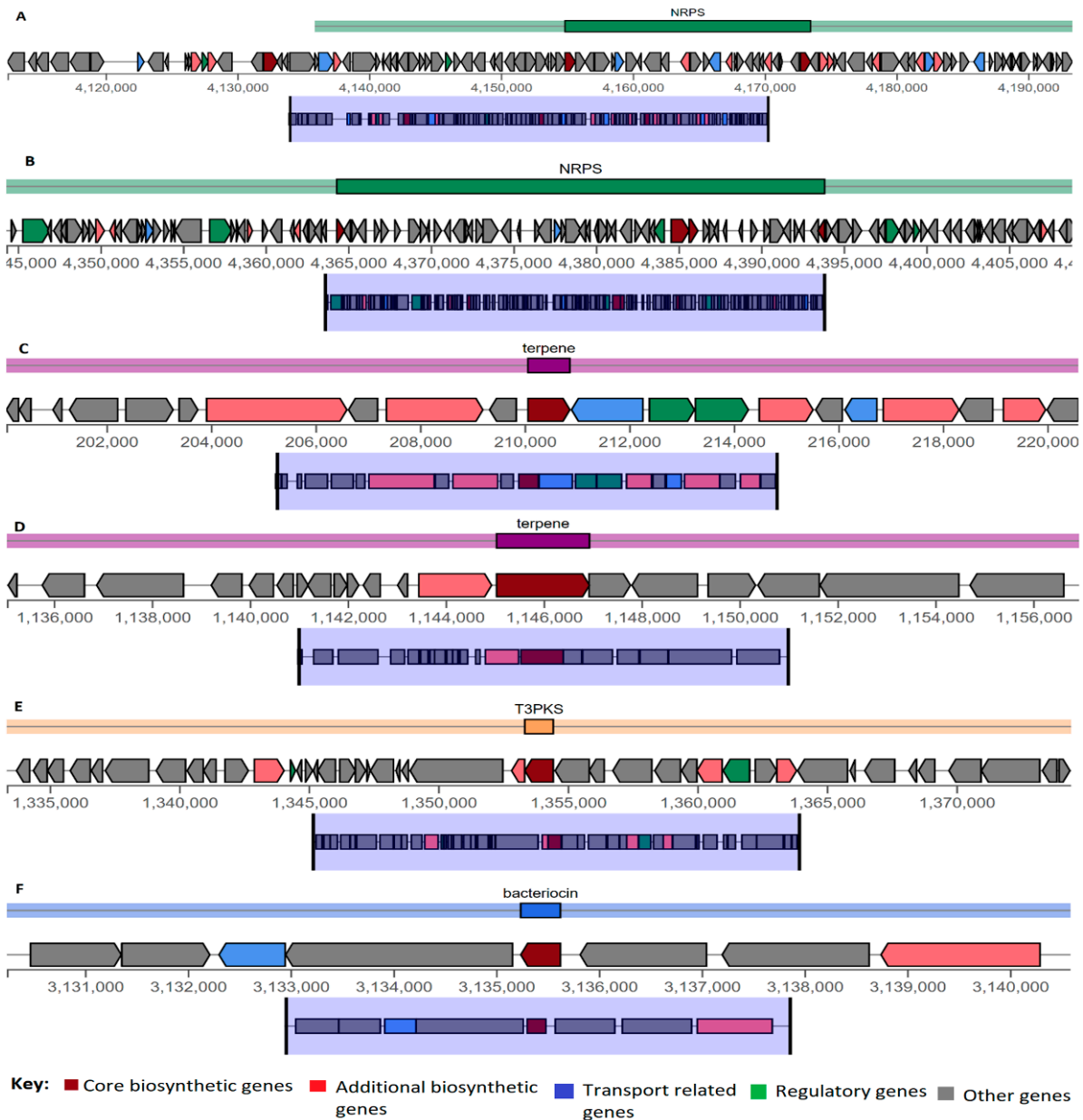


Figure 4. Organization of putative novel BGCs coding for: (A) bogorol A (NRPS); (B) surfactin (NRPS); (C) terpene; (D) terpene; (E) type 3 polyketide (T3PK); (F) RiPP (Bacteriocin), in *B. subtilis* RS10 genome.

3.6.2. Phytohormone and Siderophore Biosynthesis

Phytohormone, cytokinin encoding cluster consisting of *recA* and *recX* genes are found in *B. subtilis* RS10 genome (Supplementary File S3 Table S1). Additionally, the lysin motif domain (*lysM*) and the complete biosynthetic pathway of tryptophan (L-TRP) (*trpABCD*) were found in RS10 genome (Supplementary File S3 Table S1). The strain RS10 genome carries several genes related to siderophore biosynthesis, binding, and transport such as *dhbABCF* and *yclNOPQ* (Supplementary File S3 Table S2). The in vitro assay also confirmed the siderophore production by *B. subtilis* RS10 (Figure 1B). The RS10 genome also harbors genes associated with the shikimate pathway (Supplementary File S3 Table S2).

3.6.3. Lytic Enzymes and Volatile Organic Compounds

The genome of *B. subtilis* RS10 contains genes such as *lipAC*, *htrBC*, and *egIS/bgIS*, encoding for lipases, proteases, and glucanases, respectively (Supplementary File S3 Table S2). In addition, the genes *pl* and *ytpA* were found which are involved in pectate lyase and bacilycin biosynthesis, respectively. Furthermore, the genes associated with acetoin and 2,3-butanediol synthesis such as acetolactate synthase (*alsS*), acetolactate decarboxylase (*budA*), and acetoin dehydrogenase (*acoABCR*) were identified in the RS10 genome (Supplementary File S3 Table S2).

3.6.4. Abiotic Stress-Related Genes

Genome mining of strain RS10 revealed several genes associated with osmoprotectants and abiotic stress tolerance including high salinity and oxidative stress. The strain RS10 contains genes encoding for K⁺ uptake which is involved in early response against osmotic stress [25] and transporters genes (*ktrAD*, *kimA*), Trk system (*trkA*), and K⁺ channel (*kbFO*) (Supplementary File S3 Table S3).

The TreP pathway for trehalose biosynthesis along with regulator (*treR*) were found in *B. subtilis* strain RS10 genome (Supplementary File S3 Table S3). In the present investigation, the glycine betaine biosynthesis gene *betAB* and transporter gene *opuCD* were also detected in RS10 genome (Supplementary File S3 Table S3). Furthermore, the genes associated with inositol synthesis (*iolGIUXW*) and transport (*iolTF*) were also identified. The enzymes involved in hydrolytic and proteolytic activities against oxidative stress such as hydroperoxide reductase (*ahpCF*) and superoxide dismutase were identified in *B. subtilis* RS10 genome. In addition, the genes associated with the detoxification of free radicals by flavohemoprotein deoxygenase (*hmpA*) and nitric oxide sensor (*nsrR*) were detected. Several copies of general and universal stress genes (*yfkM* and *yugI*) were also found. In addition to these, numerous chaperons (*hemW*, *dnaK*, *dnaJ*, and *csaA*) and two-component system protein-encoding genes (*yycI*, *yesMN*, *yfiR*, *lrrK*, *yxjL*, and *yxdKJ*) to rapidly sense and adjust to the external environment were identified in the RS10 genome (Supplementary File S3 Table S3).

3.6.5. Chemotaxis and Colonization

The genome analysis revealed genes associated with flagellar biosynthesis and chemotaxis. Genes found in RS10 genome encoding for flagella structural component included *flhABF*, *fliEFGJHIKQRLMYZ*, *flgBCGD*, and *motAB* (Supplementary File S3 Table S4). Furthermore, genes associated with chemotaxis such as methyl-accepting chemotaxis protein (*tlpAB* and *mcpABC*) and two-component system chemotaxis protein (*cheAVYWD*) were detected in the RS10 genome.

Additionally, strain RS10 contains all genes associated with biofilm formation and regulation (Supplementary File S3 Table S4) which is in line with the in vitro biofilm formation. The genome of RS10 also contains integrase/recombinase encoding genes (*xerCD*) which assist the strain to colonize plant root. The genome also encodes proteins involved in plant root surface adhesion such as prepilin peptidase and prepilin terminal cleavage (*ppdD*), cellulase, and exopolysaccharide (*epsG*) (Supplementary File S3 Table S4).

The internalization of plant growth-promoting bacteria into the host occurs via tissue damage and the intact plant epidermis cells require active cell wall degrading enzymes such as hemicellulase, cellulase, and pectinase. The genome of RS10 contained genes encoding cellulase (*celB*) and pectinase (*pelC*), however, the hemicellulose encoding gene was not detected. Furthermore, pectinase transcriptional regulator gene *kdgR* was also found in the RS10 genome.

The genes responsible for hydrogen sulfide biosynthesis (*cysCHNP*) were determined in the *B. subtilis* RS10 genome. Several genes, associated with urea degradation and transport including *ureABC*, sulfate reduction and transport, as well as sulfonate degradation and transport were found in RS10 genome (Supplementary File S3 Table S5). The presence of *ssuD* genes encoding for alkanesulfonate monooxygenase suggests that the strain RS10

prominently obtains sulfite by degrading sulfonates. We also identified *gabD* and *gabP* genes that are involved in the biosynthesis of disease suppressing gamma-aminobutyric acid (GABA).

3.7. Pan- and Core-Genome Analysis

To understand the pan-/core-genome of *B. subtilis* 139 complete genomes were analyzed. The number of genes and distribution of gene families are shown in Figure 5C,D, respectively. The genome of *B. subtilis* RS10 consists of 1174 conserved genes (core-genome) and 2770 accessory genes. In total, 1525 strain-specific and 986 exclusively absent genes were identified (Supplementary File S4). The number of unique genes in all 139 strains ranges from 0 to 476. While, the strain J-5 and the newly sequenced strain RS10 comprise the highest number of unique genes ie 476 and 86, respectively (Figure 5C). The functional categories of core, accessory, and strain-specific genes were observed to be highly diverse (Figure 5B,D). The deduced power-fit curve equation ($f(x) = 5329.33 \cdot x^{0.1634}$) showed that the pan-genome is still open but may be closed soon. Moreover, the presumed exponential curve equation ($f_1(x) = 3081.85 \cdot e^{-0.009047x}$) showed that the extrapolation curve is abrupt towards down when the 65th genome is added and followed by a slight slop reaching a minimum when 139th genome is added (Figure 5A).

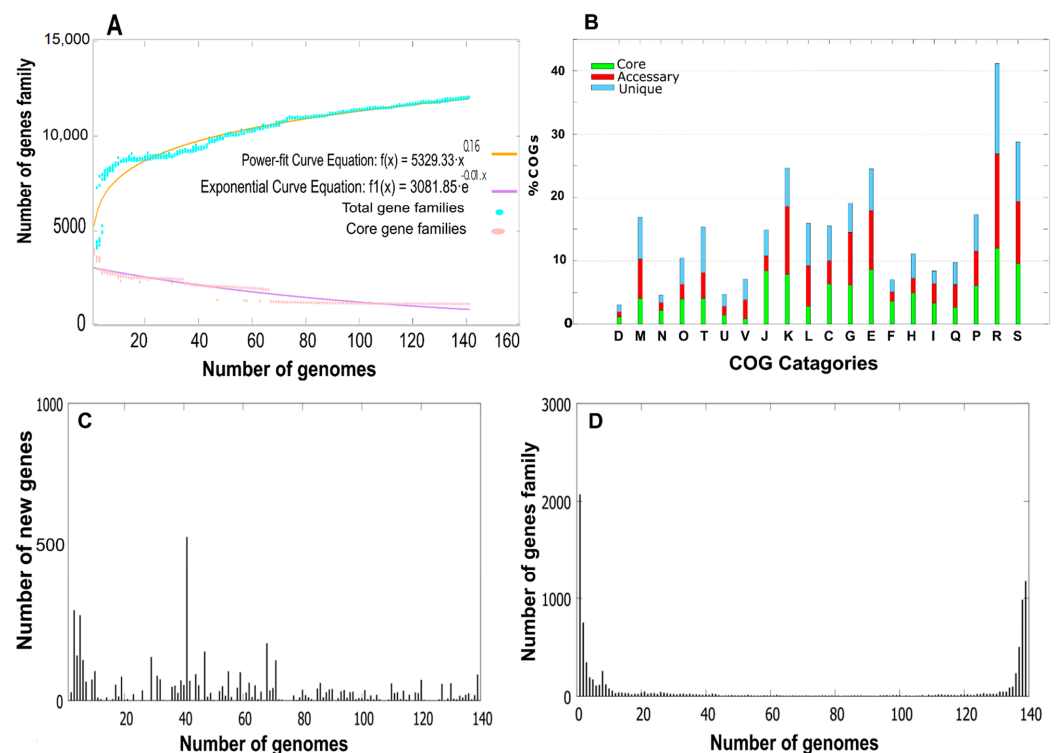


Figure 5. Mathematical extrapolation of the pan-core genome of 139 *B. subtilis* strains: (A) The core-pan genome curve; (B) COG distribution in the core genome, accessory, and unique genome pool. D, Cell division; M, Cell wall/membrane biosynthesis; N, Cell motility; O, post translational modifications; T, signal transduction, U, Intracellular trafficking and transport; V, Defense; J, Translation; K, Transcription; L, Replication and repair; C, Energy production; G, Carbohydrate metabolism and transport; E, Aminoacid metabolism and transport; F, Nucleotide metabolism and transport; H, Coenzyme metabolism and transport; I, Lipid metabolism and transport; Q, Secondary metabolites biosynthesis; P, Inorganisc ions metabolism and transport; R, General function prediction only; S, Function unknown; (C) addition of new genes to each genome; (D) distribution of gene families.

The core-genome phylogenetic tree was constructed based on 1174 concatenated core-genome proteins. The strain RS10 clustered with related *B. subtilis* strains SRCM102756,

SRCM102753, SRCM104008, SRCM104011, PR10, and GDJK2 in clade II (Figure 6). The closest relative of the strain RS10 is *B. subtilis* SRCM102756 which has also antimicrobial activity and was isolated from soy sauce Korea.

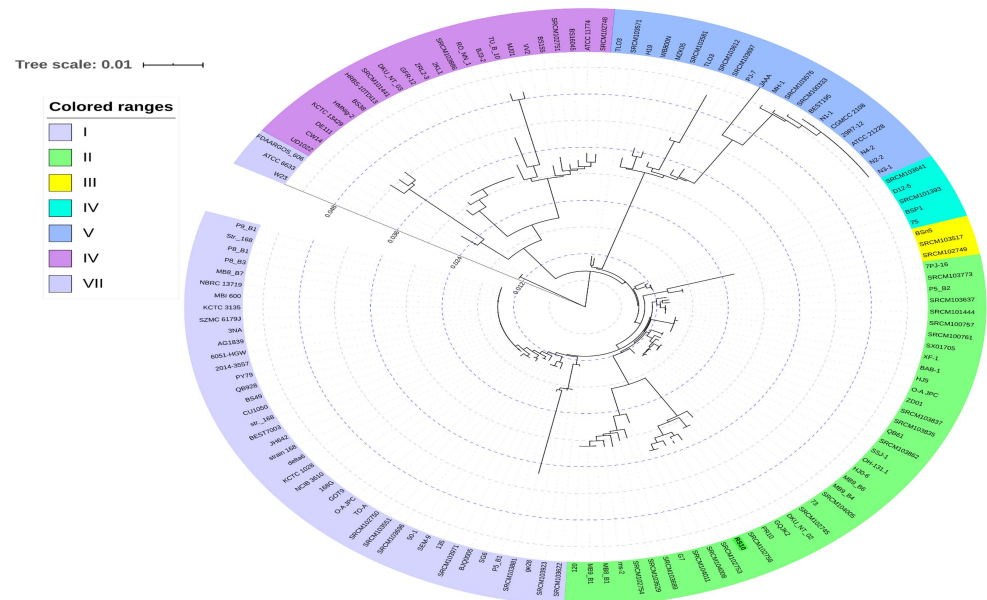


Figure 6. The evolutionary history was inferred using the Maximum Likelihood method and JTT matrix-based model. The tree with the highest log likelihood (-122314.01) is shown. Initial tree(s) for the heuristic search were obtained automatically by applying Neighbor-Join and BioNJ algorithms to a matrix of pairwise distances estimated using a JTT model, and then selecting the topology with a superior log-likelihood value. The tree is drawn to scale, with branch lengths measured in the number of substitutions per 100 sites.

4. Discussion

Chemical fertilizers, herbicides, and pesticides are hazardous and cause severe environmental problems that have made it necessary to search for a substitute to replace the chemical strategies [26]. The bacterial community associated with plant rhizosphere is the focus of research to understand and explore their role in plant growth promotion and disease control. The *B. subtilis* species prominently found in the rhizosphere, having remarkable metabolic capabilities. The secondary metabolites produced by *B. subtilis* has a profound effect on bacterial and fungal growth [27]. The current study demonstrates the antimicrobial, in vitro plant growth-promoting traits and secondary metabolites profile of newly isolated *B. subtilis* strain RS10 isolated from the rhizosphere. The strain RS10 showed broad-spectrum antimicrobial activity which was in agreement with the earlier study [28,29] where *Bacillus* sp. inhibited the growth of multiple bacterial strains and showed maximum activity against *S. aureus*. The genome assembly results of RS10 are in line with those reported previously for *B. subtilis* genomes [30,31]. The genome showed some gaps in corresponding regions to genes coding for NRPS and prophages. These gaps may be due to difficulties to the assembling tool to work with repeating strings [32].

PGPB have been reported to promote plant growth via various mechanisms including lytic enzyme and siderophore biosynthesis [33], nitrogen fixation [34], phosphate solubilization [35], biofilm formation [36], and phytohormone production [37], and also by the synthesis of antimicrobial secondary metabolite [38]. In the present study, the strain RS10 showed the ability to produce lytic enzymes including protease, amylase, and cellulase on agar plates that was also verified by the determination of genes associated with protease, cellulase, and amylase synthesis in RS10 genome. The rhizospher organisms which produce protease, cellulase, and amylase not only help in organic matter decomposition but also induce plant growth, suppress soil born pathogen, and maintain soil ecology and fertil-

ity [39]. Cellulase depolymerizes cellulose into fermentable sugar and also assist bacteria to penetrate host plant cells. Previous studies where plant growth-promoting *Bacillus* strains CNPo 2477 and BPSAC6 were isolated from soil were also shown to produce proteases and cellulases [39,40]. In addition to lytic enzymes, the antimicrobial secondary metabolites also contribute to biocontrol activity. Genome mining of RS10 revealed numerous BGCs for antimicrobial secondary metabolites including surfactin, fengycins, bacillibactin, bacilysin, terpene, and bogorol. The presence of these BGCs in RS10 genome corroborated the in vitro antimicrobial activity. The fengycin and surfactin were previously reported to inhibit the growth of filamentous fungi and bacteria [41]. Fan et al. also confirmed that surfactin is crucial for biocontrol activity of *B. subtilis* 9407. Bacillibactin acts as a siderophore and assists the producer organism to compete with the neighboring organism in an iron-deficient environment. Siderophores are of dual interest as they prevent the colonization of plant–pathogen and also act as a source of assimilable iron for plants [42]. Similarly, bacilysin exhibits broad-spectrum antimicrobial activities against bacteria as well as fungi [41]. A new Bogorol A encoding gene cluster exhibiting no similarity with a known cluster is first time identified in *B. subtilis* RS10 genome. The BGC coding for bogorol A is completely missing in reference strain *B. subtilis* 168 (Table 1). Bogorol is a family of antibiotics previously isolated from marine *Bacillus* sp. inhibiting the growth of methicillin-resistant *S. aureus* and *E. coli* [43]. Terpene is generally considered to be a fungal and plant natural product. However, recently, it was reported that bacterial genomes also harbor gene cluster encoding for terpenes [44]. We identified two unique clusters coding for terpenes, exhibited no similarity with a known cluster. In addition, one BGC each for T3PKS and bacteriocin were also found unique, and thus suggested to produce novel bioactive compounds. These BGCs are potentially responsible to antagonize the growth of indicator strains, as reported previously by several authors [31,45,46].

The genes associated with plant growth-promoting traits were annotated and metabolic predictions were achieved. We identified that *B. subtilis* strain RS10 carries genes related to phosphate solubilization, phytohormone biosynthesis, chemotaxis and colonization, volatile organic compounds biosynthesis, and abiotic stress. The strain RS10 lack *nif* operon required for nitrogen fixation. However, the strain carries genes encoding for molybdopterin biosynthesis adpter protein (*mob* and *moeB*) and cofactor biosynthesis (*moaABCDE*), which may be an artifact of nitrogen fixation gene cluster, as suggested previously [47].

The presence of siderophore biosynthesis and phosphate solubilization machinery in *B. subtilis* RS10 genome biochemically corroborated with its in vitro activities. These features are associated with iron assimilation and induce systemic resistance in plants [48]. Additionally, the lysin motif domain (*lysM*) was identified which is involved in the signaling of root nodule symbiosis between plant and bacteria [49]. The plant hormones cytokinin and L-tryptophan identified in RS10 are involved in several stages of plant growth and development such as apical dominance, cell division, cell elongation, and tissue differentiation [50]. Cytokinin is an active precursor of the phytohormone auxin and its availability increases the level of auxin in plants [1]. Previously, various studies demonstrated the positive response of L-tryptophan in enhancing plant growth and productivity [51–53]. Two volatile organic compounds coding genes including acetoin and butanediol were found in the RS10 genome, which was earlier reported to act as antibiotics and antagonize the growth of phytopathogens and facilitate nutrients absorption [54,55]. The *pl* gene coding for pectate lyase was detected. The pectate lyase was previously determined in plant growth-promoting *F. saprophytica* and *F. elaeagni* [56]. It has also been found in pathogenic bacteria and is known to degrade host tissue during infection [57]. The exact function of *pl* gene is debated in PGPB, since we hypothesis that it is likely to be involved in the initiation of bacteria–plant interaction. Recently, several studies indicated that swarming motility facilitated bacteria to move towards plant roots [58–60] and biofilm support root colonization [61]. Swarming motility is a result of swinging flagellum coding by *flg* and *fli* operon [62]. The *eps* operon is responsible for synthesizing core components

of the biofilm [61]. The presence of these operons in *B. subtilis* RS10 implies its potential to effectively migrate and colonize in plant roots.

Abiotic stress such as osmotic stress or high salinity is hostile to plant growth and development, leading to huge crop yield losses worldwide. The strain RS10 genome harbors numerous genes related to abiotic stress tolerance which is pertinent to PGPB to promote plant growth in osmotic stress and high salinity environment. The use of such stress mitigating PGPB is a newly emerging strategy for improving crop quality and yield [63]. However, to successfully adopt this strategy the knowledge of molecular and physiological mechanisms which direct PGPB-plant interaction is essentially required.

Pan-genome analysis is used to explore core, pan, and unique genes and to assess genomic diversity in a specific species [64]. In the present study, for the first time, we conducted a comprehensive pan-/core-genome analysis of all complete genomes ($n = 139$) available in public databases that revealed an open pan-genome and a core genome consisting of 1174 genes. Previously, a pan-/core-genome analysis of *B. subtilis* and *B. amyloliquifaciens* ($n = 31$) was performed and predicted an open pan-genome with a core genome of 2,409 genes [65]. The lower number of core genes in our study is likely due to the higher number of genomes in a dataset. Core and strain-specific genes in each strain show significant differences in genomic fingerprints, which is probably due to several HGT events. A previous study revealed that HGT is an important feature for genome plasticity for rhizosphere colonization [66]. An earlier study reported that the bacterial strains acquired from genomic islands via HGT executed better symbiotic nitrogen fixation competency than other related strains [67]. Our functional analysis of core and strain-specific genes show that several strain-specific genes are associated with prophages, replication, recombination and repair (L), and general function category (R), which suggest the importance of core genes in the identification of *B. subtilis*. These results are in agreement with an earlier study where pan-genome analysis was conducted on the core genes data of several *Bacillus* species to analyze them in fermented food microbiome [68].

The phylogenetic tree constructed based on core-genome indicates that the strains isolated from rhizosphere and having antibacterial activity are distinguished from others which are isolated from different sources such as food, feces, and gut. These findings suggest that some important changes in these strains have occurred during adaptation to a specific habitat. These changes might be the result of co-evolution with plants [69]. This implies that a particular habitat, such as a plant-associated habitat has a profound effect on HGT and highlights a consistency between the nucleotide sequences and hierarchal clustering [70] which is in agreement with a study that demonstrated HGT in various *streptococcus* species had the same shared habitat [71]. In the phylogenetic tree, mostly the clade is consistent with their habitat but there are few exemptions. For instance, the strains SRCM102750, SRCM102753, SRCM103576, and SRCM102748 were all isolated from different fermented foods but shared clades with almost all groups except the spizizenii group (Figure 6). The reason for this inconsistency is unclear; to some extent, the subsequent mutation in the laboratory might lead to this contradiction but in fact, the genetic mutation that occurs during or after domestication appears to be limited. The strains which are isolated from a specific niche are not guaranteed to be adapted with that particular habitat.

5. Conclusions

Plant roots harbor a wide range of bacteria which make symbiotic relations with the plant by providing nutritional, fitness, and stress tolerance support. The strain RS10 genome carries all of the signature genes which are associated with the plant growth-promoting capabilities. The in vitro assay confirms the antagonistic and plant growth-promoting capabilities. The genome analysis reveal that *B. subtilis* RS10 has the capacity to solubilize inorganic phosphate, synthesis hydrogen sulfide, and produce siderophore and phytohormones. In addition, genome mining also confirms its ability to withstand various stress conditions such as oxidative and antibiotic stress which is perpetrated in the rhizospheric environment. Furthermore, the strain RS10 encodes the necessary arse-

nal critical for chemotaxis and adhesion to plant root surfaces. The strain also contains genes for colonization and metabolic versatility to use root exudate. Together, the present investigation provides important insight into the genomic diversity and remarkable plant growth-promoting potential of strain RS10 for sustainable agriculture. However, additional investigation is required to identify these interesting bioactive metabolites and their potential as PGP strain in the field.

Supplementary Materials: The following are available online at <https://www.mdpi.com/article/10.3390/agriculture11121273/s1>, Supplementary File S1 Table S1: Antagonistic and plant growth-promoting traits in rhizosphere strains isolated from various plant roots, Supplementary File S2 Table S1: Detail of genomic islands identified in *B. subtilis* RS10 genome, File S2 Table S2: Prophage regions identified in *B. subtilis* RS10 genome, Supplementary File S3 Table S1: Plant growth-promoting (direct mechanisms) related genes in *B. subtilis* RS10, File S3 Table S2: Plant growth-promoting (indirect mechanisms) related genes in *B. subtilis* RS10, File S3 Table S3: Abiotic stress related genes in *B. subtilis* RS10, File S3 Table S4: Chemotaxis, motility and colonization related genes in *B. subtilis* RS10, File S3 Table S5: Others plant growth-promoting genes in *B. subtilis* RS10, Supplementary File S4 Table S1: Pan-core genome analysis of *B. subtilis* ($n = 139$) complete genomes.

Author Contributions: Conceptualization and study designing, S.I. and H.A.J.; software, writing—original draft preparation, visualization, S.I; formal analysis and writing—review and editing N.U. and S.I.; supervision and resources, H.A.J. All authors have read and agreed to the published version of the manuscript.

Funding: The current research was supported by the University (NUST) student research fund and did not received any external funding.

Institutional Review Board Statement: Not applicable.

Informed Consent Statement: Not applicable.

Data Availability Statement: The whole-genome sequence of *B. subtilis* strain RS10 has been submitted to NCBI, GenBank under the accession number CP046860.1.

Acknowledgments: We acknowledge Muhammad Faraz Bhatti (PI. Mycoviruses laboratory) who provided the phytopathogenic fungi.

Conflicts of Interest: The authors declare no conflict of interest.

References

1. Ahemad, M.; Kibret, M. Mechanisms and applications of plant growth promoting rhizobacteria: Current perspective. *J. King Saud. Univ. Sci.* **2014**, *26*, 39–54. [[CrossRef](#)]
2. Lugtenberg, B.; Kamilova, F. Plant-Growth-Promoting Rhizobacteria. *Annu. Rev. Microbiol.* **2009**, *63*, 541–556. [[CrossRef](#)] [[PubMed](#)]
3. Setlow, P. Spores of *Bacillus subtilis*: Their resistance to and killing by radiation, heat and chemicals. *J. Appl. Microbiol.* **2006**, *101*, 514–525. [[CrossRef](#)] [[PubMed](#)]
4. Zhao, X.; Kuipers, O.P. Identification and classification of known and putative antimicrobial compounds produced by a wide variety of Bacillales species. *BMC Genom.* **2016**, *17*, 882. [[CrossRef](#)] [[PubMed](#)]
5. Caulier, S.; Nannan, C.; Gillis, A.; Licciardi, F.; Bragard, C.; Mahillon, J. Overview of the antimicrobial compounds produced by members of the *Bacillus subtilis* group. *Front. Microbiol.* **2019**, *10*, 302. [[CrossRef](#)]
6. Bais, H.P.; Fall, R.; Vivanco, J.M. Biocontrol of *Bacillus subtilis* against infection of *Arabidopsis* roots by *Pseudomonas syringae* is facilitated by biofilm formation and surfactin production. *Plant Physiol.* **2004**, *134*, 307–319. [[CrossRef](#)] [[PubMed](#)]
7. Romero, D.; de Vicente, A.; Rakotoaly, R.H.; Dufour, S.E.; Veening, J.-W.; Arrebola, E.; Cazorla, F.M.; Kuipers, O.P.; Paquot, M.; Pérez-García, A. The iturin and fengycin families of lipopeptides are key factors in antagonism of *Bacillus subtilis* toward *Podospaera fusca*. *Mol. Plant Microbe Interact.* **2007**, *20*, 430–440. [[CrossRef](#)] [[PubMed](#)]
8. Chen, X.H.; Scholz, R.; Borriss, M.; Junge, H.; Mögel, G.; Kunz, S.; Borriss, R. Difficidin and bacilysin produced by plant-associated *Bacillus amyloliquefaciens* are efficient in controlling fire blight disease. *J. Biotechnol.* **2009**, *140*, 38–44. [[CrossRef](#)]
9. Xing, Z.; Wu, X.; Zhao, J.; Zhao, X.; Zhu, X.; Wang, Y.; Fan, H.; Chen, L.; Liu, X.; Duan, Y. Isolation and identification of induced systemic resistance determinants from *Bacillus simplex* Sneb545 against *Heterodera glycines*. *Sci. Rep.* **2020**, *10*, 11586. [[CrossRef](#)]
10. Zhou, C.; Zhu, J.; Qian, N.; Guo, J.; Yan, C. *Bacillus subtilis* SL18r Induces Tomato Resistance Against *Botrytis cinerea*, Involving Activation of Long Non-coding RNA, MSTRG18363, to Decoy miR1918. *Front. Plant Sci.* **2021**, *11*, 2317. [[CrossRef](#)]

11. Tahir, H.A.S.; Gu, Q.; Wu, H.; Raza, W.; Hanif, A.; Wu, L.; Colman, M.V.; Gao, X. Plant Growth Promotion by Volatile Organic Compounds Produced by *Bacillus subtilis* SYST2. *Front. Microbiol.* **2017**, *8*, 171. [[CrossRef](#)]
12. Wäli, P.P.; Wäli, P.R.; Saikkonen, K.; Tuomi, J. Is the pathogenic ergot fungus a conditional defensive mutualist for its host grass? *PLoS ONE* **2013**, *8*, e69249. [[CrossRef](#)] [[PubMed](#)]
13. Schöniger, S.; Roschanski, N.; Rösler, U.; Vidovic, A.; Nowak, M.; Dietz, O.; Wittenbrink, M.M.; Schoon, H.-A. Prototheca species and *Pithomyces chartarum* as Causative Agents of Rhinitis and/or Sinusitis in Horses. *J. Comp. Pathol.* **2016**, *155*, 121–125. [[CrossRef](#)] [[PubMed](#)]
14. Iqbal, S.; Vollmers, J.; Janjua, H.A. Genome Mining and Comparative Genome Analysis Revealed Niche-Specific Genome Expansion in Antibacterial *Bacillus pumilus* Strain SF-4. *Genes* **2021**, *12*, 1060–1079. [[CrossRef](#)] [[PubMed](#)]
15. Iqbal, S.; Vohra, M.S.; Janjua, H.A. Whole-genome sequence and broad-spectrum antibacterial activity of *Chryseobacterium cucumeris* strain MW-6 isolated from the Arabian Sea. *3 Biotech* **2021**, *11*, 489. [[CrossRef](#)]
16. O'Toole, G.A. Microtiter dish biofilm formation assay. *J. Vis. Exp.* **2011**, 2437. [[CrossRef](#)]
17. Kasana, R.C.; Salwan, R.; Dhar, H.; Dutt, S.; Gulati, A. A rapid and easy method for the detection of microbial cellulases on agar plates using gram's iodine. *Curr. Microbiol.* **2008**, *57*, 503–507. [[CrossRef](#)]
18. Arora, N.K.; Verma, M. Modified microplate method for rapid and efficient estimation of siderophore produced by bacteria. *3 Biotech* **2017**, *7*, 381. [[CrossRef](#)]
19. Bolger, A.M.; Lohse, M.; Usadel, B. Trimmomatic: A flexible trimmer for Illumina sequence data. *Bioinformatics* **2014**, *30*, 2114–2120. [[CrossRef](#)]
20. Bankevich, A.; Nurk, S.; Antipov, D.; Gurevich, A.A.; Dvorkin, M.; Kulikov, A.S.; Lesin, V.M.; Nikolenko, S.I.; Pham, S.; Pribelski, A.D.; et al. SPAdes: A new genome assembly algorithm and its applications to single-cell sequencing. *J. Comput. Biol.* **2012**, *19*, 455–477. [[CrossRef](#)]
21. Tsai, I.J.; Otto, T.D.; Berriman, M. Improving draft assemblies by iterative mapping and assembly of short reads to eliminate gaps. *Genome Biol.* **2010**, *11*, R41. [[CrossRef](#)] [[PubMed](#)]
22. Tatusova, T.; Dicuccio, M.; Badretdin, A.; Chetvermin, V.; Nawrocki, E.P.; Zaslavsky, L.; Lomsadze, A.; Pruitt, K.D.; Borodovsky, M.; Ostell, J. NCBI prokaryotic genome annotation pipeline. *Nucleic Acids Res.* **2016**, *44*, 6614–6624. [[CrossRef](#)] [[PubMed](#)]
23. Chaudhari, N.M.; Gupta, V.K.; Dutta, C. BPGA-an ultra-fast pan-genome analysis pipeline. *Sci. Rep.* **2016**, *6*, 24373. [[CrossRef](#)] [[PubMed](#)]
24. Kumar, S.; Stecher, G.; Li, M.; Nnyaz, C.; Tamura, K. MEGA X: Molecular evolutionary genetics analysis across computing platforms. *Mol. Biol. Evol.* **2018**, *35*, 1547–1549. [[CrossRef](#)] [[PubMed](#)]
25. Bremer, E.; Krämer, R. Responses of Microorganisms to Osmotic Stress. *Annu. Rev. Microbiol.* **2019**, *73*, 313–334. [[CrossRef](#)] [[PubMed](#)]
26. Glick, B.R.; Todorovic, B.; Czarny, J.; Cheng, Z.; Duan, J.; McConkey, B. Promotion of Plant Growth by Bacterial ACC Deaminase. *CRC Crit. Rev. Plant Sci.* **2007**, *26*, 227–242. [[CrossRef](#)]
27. Kiesewalter, H.T.; Lozano-Andrade, C.N.; Wibowo, M.; Strube, M.L.; Maroti, G.; Snyder, D.; Jørgensen, T.S.; Larsen, T.O.; Cooper, V.S.; Weber, T.; et al. Genomic and Chemical Diversity of *Bacillus subtilis* Secondary Metabolites against Plant Pathogenic Fungi. *mSystems* **2021**, *6*, e00770-20. [[CrossRef](#)]
28. Iqbal, S.; Rahman, H.; Begum, F.; Sajid, I.; Qasim, M. Characterization and Antibacterial Activity of *Bacillus subtilis* MK-4 Isolated from Southern Area of Pakistan. *Int. J. Mol. Microbiol.* **2019**, *2*, 41–50.
29. Gislin, D.; Sudarsanam, D.; Raj, G.A.; Baskar, K. Antibacterial activity of soil bacteria isolated from Kochi, India and their molecular identification. *J. Genet. Eng. Biotechnol.* **2018**, *16*, 287–294. [[CrossRef](#)]
30. Rahimi, T.; Niazi, A.; Deihimi, T.; Taghavi, S.M.; Ayatollahi, S.; Ebrahimie, E. Genome annotation and comparative genomic analysis of *Bacillus subtilis* MJ01, a new bio-degradation strain isolated from oil-contaminated soil. *Funct. Integr. Genom.* **2018**, *18*, 533–543. [[CrossRef](#)]
31. Franco-Sierra, N.D.; Posada, L.F.; Santa-María, G.; Romero-Tabarez, M.; Villegas-Escobar, V.; Álvarez, J.C. *Bacillus subtilis* EA-CB0575 genome reveals clues for plant growth promotion and potential for sustainable agriculture. *Funct. Integr. Genom.* **2020**, *20*, 575–589. [[CrossRef](#)] [[PubMed](#)]
32. Nederbragt, A.J.; Rounge, T.B.; Kausrud, K.L.; Jakobsen, K.S. Identification and Quantification of Genomic Repeats and Sample Contamination in Assemblies of 454 Pyrosequencing Reads. *Sequencing* **2010**, *2010*, 782465. [[CrossRef](#)]
33. Lodewyckx, C.; Vangronsveld, J.; Porteous, F.; Moore, E.R.B.; Taghavi, S.; Mezgeay, M.; van der Lelie, D. Endophytic Bacteria and Their Potential Applications. *CRC Crit. Rev. Plant Sci.* **2002**, *21*, 583–606. [[CrossRef](#)]
34. Stéphane, C.; Birgit, R.; Angela, S.; Jerzy, N.; Christophe, C.; Essaid, A.B. Endophytic Colonization of *Vitis vinifera* L. by Plant Growth-Promoting *Bacterium Burkholderia* sp. Strain PsJN. *Appl. Environ. Microbiol.* **2005**, *71*, 1685–1693. [[CrossRef](#)]
35. Rosenblueth, M.; Martínez-Romero, E. Bacterial endophytes and their interactions with hosts. *Mol. Plant Microbe Interact.* **2006**, *19*, 827–837. [[CrossRef](#)]
36. Tariq, M.; Hameed, S.; Yasmeen, T.; Zahid, M.; Zafar, M. Molecular characterization and identification of plant growth promoting endophytic bacteria isolated from the root nodules of pea (*Pisum sativum* L.). *World J. Microbiol. Biotechnol.* **2014**, *30*, 719–725. [[CrossRef](#)]

37. Lee, S.; Flores-Encarnación, M.; Contreras-Zentella, M.; Garcia-Flores, L.; Escamilla, J.E.; Kennedy, C. Indole-3-acetic acid biosynthesis is deficient in *Gluconacetobacter diazotrophicus* strains with mutations in cytochrome c biogenesis genes. *J. Bacteriol.* **2004**, *186*, 5384–5391. [[CrossRef](#)]
38. Kavamura, V.N.; Santos, S.N.; da Silva, J.L.; Parma, M.M.; Ávila, L.A.; Visconti, A.; Zucchi, T.D.; Taketani, R.G.; Andreote, F.D.; de Melo, I.S. Screening of Brazilian cacti rhizobacteria for plant growth promotion under drought. *Microbiol. Res.* **2013**, *168*, 183–191. [[CrossRef](#)] [[PubMed](#)]
39. Passari, A.K.; Mishra, V.K.; Leo, V.V.; Gupta, V.K.; Singh, B.P. Phytohormone production endowed with antagonistic potential and plant growth promoting abilities of culturable endophytic bacteria isolated from *Clerodendrum colebrookianum* Walp. *Microbiol. Res.* **2016**, *193*, 57–73. [[CrossRef](#)] [[PubMed](#)]
40. Szilagyi-Zecchin, V.J.; Ikeda, A.C.; Hungria, M.; Adamoski, D.; Kava-Cordeiro, V.; Glienke, C.; Galli-Terasawa, L.V. Identification and characterization of endophytic bacteria from corn (*Zea mays* L.) roots with biotechnological potential in agriculture. *AMB Express* **2014**, *4*, 26. [[CrossRef](#)]
41. Seydlová, G.; Svobodová, J. Review of surfactin chemical properties and the potential biomedical applications. *Cent. Eur. J. Med.* **2008**, *3*, 123–133. [[CrossRef](#)]
42. Ahmed, E.; Holmström, S.J.M. Siderophores in environmental research: Roles and applications. *Microb. Biotechnol.* **2014**, *7*, 196–208. [[CrossRef](#)] [[PubMed](#)]
43. Barsby, T.; Kelly, M.T.; Gagné, S.M.; Andersen, R.J. Bogorol A Produced in Culture by a Marine *Bacillus* sp. Reveals a Novel Template for Cationic Peptide Antibiotics. *Org. Lett.* **2001**, *3*, 437–440. [[CrossRef](#)] [[PubMed](#)]
44. Yamada, Y.; Kuzuyama, T.; Komatsu, M.; Shin-ya, K.; Omura, S.; Cane, D.E.; Ikeda, H. Terpene synthases are widely distributed in bacteria. *Proc. Natl. Acad. Sci. USA* **2015**, *112*, 857–862. [[CrossRef](#)] [[PubMed](#)]
45. Fan, B.; Wang, C.; Song, X.; Ding, X.; Wu, L.; Wu, H.; Gao, X.; Borriss, R. *Bacillus velezensis* FZB42 in 2018: The Gram-Positive Model Strain for Plant Growth Promotion and Biocontrol. *Front. Microbiol.* **2018**, *9*, 2491. [[CrossRef](#)] [[PubMed](#)]
46. Villegas-Escobar, V.; Ceballos, I.; Mira, J.J.; Argel, L.E.; Orduz Peralta, S.; Romero-Tabarez, M. Fengycin C Produced by *Bacillus subtilis* EA-CB0015. *J. Nat. Prod.* **2013**, *76*, 503–509. [[CrossRef](#)]
47. Demtröder, L.; Narberhaus, F.; Masepohl, B. Coordinated regulation of nitrogen fixation and molybdate transport by molybdenum. *Mol. Microbiol.* **2019**, *111*, 17–30. [[CrossRef](#)]
48. Aznar, A.; Dellagi, A. New insights into the role of siderophores as triggers of plant immunity: What can we learn from animals? *J. Exp. Bot.* **2015**, *66*, 3001–3010. [[CrossRef](#)]
49. Willmann, R.; Nürnberger, T. How plant lysin motif receptors get activated: Lessons learned from structural biology. *Sci. Signal.* **2012**, *5*, pe28. [[CrossRef](#)] [[PubMed](#)]
50. Erland, L.A.E.; Saxena, P. Auxin driven indoleamine biosynthesis and the role of tryptophan as an inductive signal in *Hypericum perforatum* (L.). *PLoS ONE* **2019**, *14*, e0223878. [[CrossRef](#)] [[PubMed](#)]
51. Hassan, T.; Bano, A. The stimulatory effects of L-tryptophan and plant growth promoting rhizobacteria (PGPR) on soil health and physiology of wheat. *J. Soil Sci. Plant Nutr.* **2015**, *15*, 190–201. [[CrossRef](#)]
52. Hussain, M.; Akhtar, M.; Asghar, H.; Ahmad, M. Growth, nodulation and yield of mash bean (*Vigna mungo* L.) as affected by Rhizobium inoculation and soil applied L-tryptophan. *Soil Environ.* **2011**, *30*, 13–17.
53. Zulqadar, S.; Arshad, M.; Naveed, M.; Hussain, A.; Nazir, Q.; Rizwan, M. Response of okra (*Abelmoschus esculentus* L.) to soil and foliar application of L-methionine. *Soil Environ.* **2015**, *34*, 180–186.
54. Sharifi, R.; Ryu, C.-M. Revisiting bacterial volatile-mediated plant growth promotion: Lessons from the past and objectives for the future. *Ann. Bot.* **2018**, *122*, 349–358. [[CrossRef](#)]
55. Loper, J.E.; Hassan, K.A.; Mavrodi, D.V.; Davis, E.W., II; Lim, C.K.; Shaffer, B.T.; Elbourne, L.D.H.; Stockwell, V.O.; Hartney, S.L.; Breakwell, K.; et al. Comparative Genomics of Plant-Associated *Pseudomonas* spp.: Insights into Diversity and Inheritance of Traits Involved in Multitrophic Interactions. *PLOS Genet.* **2012**, *8*, e1002784. [[CrossRef](#)] [[PubMed](#)]
56. Nouioui, I.; Cortés-albayay, C.; Carro, L.; Castro, J.F.; Gtari, M.; Ghodhbane-Gtari, F.; Klenk, H.-P.; Tisa, L.S.; Sangal, V.; Goodfellow, M. Genomic Insights Into Plant-Growth-Promoting Potentialities of the Genus Frankia. *Front. Microbiol.* **2019**, *10*, 1457. [[CrossRef](#)] [[PubMed](#)]
57. Marín-Rodríguez, M.C.; Orchard, J.; Seymour, G.B. Pectate lyases, cell wall degradation and fruit softening. *J. Exp. Bot.* **2002**, *53*, 2115–2119. [[CrossRef](#)]
58. Gao, S.; Wu, H.; Yu, X.; Qian, L.; Gao, X. Swarming motility plays the major role in migration during tomato root colonization by *Bacillus subtilis* SWR01. *Biol. Control* **2016**, *98*, 11–17. [[CrossRef](#)]
59. Allard-Massicotte, R.; Tessier, L.; LÚcuyer, F.; Lakshmanan, V.; Lucier, J.F.; Garneau, D.; Caudwell, L.; Vlamakis, H.; Bais, H.P.; Beauregard, P.B.; et al. *Bacillus subtilis* Early Colonization of Arabidopsis thaliana Roots Involves Multiple Chemotaxis Receptors. *MBio* **2021**, *7*, e01664-16. [[CrossRef](#)]
60. Gu, X.; Zeng, Q.; Wang, Y.; Li, J.; Zhao, Y.; Li, Y.; Wang, Q. Comprehensive genomic analysis of *Bacillus subtilis* 9407 reveals its biocontrol potential against bacterial fruit blotch. *Phytopathol. Res.* **2021**, *3*, 4. [[CrossRef](#)]
61. Verstraeten, N.; Braeken, K.; Debkumari, B.; Fauvart, M.; Fransaeer, J.; Vermant, J.; Michiels, J. Living on a surface: Swarming and biofilm formation. *Trends Microbiol.* **2008**, *16*, 496–506. [[CrossRef](#)] [[PubMed](#)]
62. Kearns, D.B. A field guide to bacterial swarming motility. *Nat. Rev. Microbiol.* **2010**, *8*, 634–644. [[CrossRef](#)] [[PubMed](#)]

63. Lephatsi, M.M.; Meyer, V.; Piater, L.A.; Dubery, I.A.; Tugizimana, F. Plant Responses to Abiotic Stresses and Rhizobacterial Biostimulants: Metabolomics and Epigenetics Perspectives. *Metabolites* **2021**, *11*, 457. [[CrossRef](#)] [[PubMed](#)]
64. Vernikos, G.; Medini, D.; Riley, D.R.; Tettelin, H. Ten years of pan-genome analyses. *Curr. Opin. Microbiol.* **2015**, *23*, 148–154. [[CrossRef](#)]
65. Zhang, N.; Yang, D.; Kendall, J.R.A.; Borriss, R.; Druzhinina, I.S.; Kubicek, C.P.; Shen, Q.; Zhang, R. Comparative Genomic Analysis of *Bacillus amyloliquefaciens* and *Bacillus subtilis* Reveals Evolutional Traits for Adaptation to Plant-Associated Habitats. *Front. Microbiol.* **2016**, *7*, 2039. [[CrossRef](#)] [[PubMed](#)]
66. Lopes, L.D.; Pereira, E.; de Silva, M.C.; Andreote, F.D. Bacterial Abilities and Adaptation Toward the Rhizosphere Colonization. *Front. Microbiol.* **2016**, *7*, 1341. [[CrossRef](#)]
67. Itakura, M.; Saeki, K.; Omori, H.; Yokoyama, T.; Kaneko, T.; Tabata, S.; Ohwada, T.; Tajima, S.; Uchiumi, T.; Honnma, K.; et al. Genomic comparison of Bradyrhizobium japonicum strains with different symbiotic nitrogen-fixing capabilities and other Bradyrhizobiaceae members. *ISME J.* **2009**, *3*, 326–339. [[CrossRef](#)]
68. Kim, Y.; Koh, I.; Young Lim, M.; Chung, W.-H.; Rho, M. Pan-genome analysis of Bacillus for microbiome profiling. *Sci. Rep.* **2017**, *7*, 10984. [[CrossRef](#)] [[PubMed](#)]
69. Hartmann, A.; Schmid, M.; van Tuinen, D.; Berg, G. Plant-driven selection of microbes. *Plant Soil* **2009**, *321*, 235–257. [[CrossRef](#)]
70. Hao, W.; Golding, G.B. The fate of laterally transferred genes: Life in the fast lane to adaptation or death. *Genome Res.* **2006**, *16*, 636–643. [[CrossRef](#)] [[PubMed](#)]
71. Richards, V.P.; Palmer, S.R.; Bitar, P.D.P.; Qin, X.; Weinstock, G.M.; Highlander, S.K.; Town, C.D.; Burne, R.A.; Stanhope, M.J. Phylogenomics and the dynamic genome evolution of the genus *Streptococcus*. *Genome Biol. Evol.* **2014**, *6*, 741–753. [[CrossRef](#)] [[PubMed](#)]